Optimized Machine Learning for Induction Motor Fault Diagnosis Using Vibration and Frequency-Domain Features

Somdavee Bhosinak
Faculty of Engineering, Mahasarakham University, Maha Sarakham, Thailand
67010361006@msu.ac.th

Sitthisak Audomsi
Faculty of Engineering, Mahasarakham University, Maha Sarakham, Thailand
67010361003@msu.ac.th

Niwat Angkawisittpan
Faculty of Engineering, Mahasarakham University, Maha Sarakham, Thailand | Electrical and Computer Engineering Research Unit, Mahasarakham University, Maha Sarakham, Thailand
niwat.a@msu.ac.th

Chonlatee Photong
Faculty of Engineering, Mahasarakham University, Maha Sarakham, Thailand | Electrical and Computer Engineering Research Unit, Mahasarakham University, Maha Sarakham, Thailand
chonlatee.p@msu.ac.th

Worawat Sa-Ngiamvibool
Faculty of Engineering, Mahasarakham University, Maha Sarakham, Thailand | Electrical and Computer Engineering Research Unit, Mahasarakham University, Maha Sarakham, Thailand
wor.nui@gmail.com (corresponding author)

Received: 28 June 2025 | Revised: 23 August 2025 | Accepted: 6 September 2025

Licensed under a CC-BY 4.0 license | Copyright (c) by the authors | *DOI: https://doi.org/10.48084/etasr.13017*

ABSTRACT

This study uses vibration signal analysis to assess and contrast several machine learning models for identifying defects in induction motors. A comprehensive dataset obtained from TDMS-format sensor recordings included seven inter-turn short circuit fault conditions and one normal state. Three experimental settings were investigated: (i) multiclass classification with basic time-domain features, (ii) binary classification using enhanced time and Fast Fourier Transform (FFT) frequency-domain features, and (iii) optimal binary classification using hyperparameter tuning and advanced boosting models. KNN, Random Forest (RF), and ensemble models (XGBoost, LightGBM, CatBoost) were trained and evaluated using accuracy, MSE, RMSE, and R^2. The results reveal that while raw time-domain features performed poorly in multiclass tasks (accuracy ~20%), significant gains were obtained utilizing FFT features and binary classification (accuracy up to 80%). Using hyperparameter tuning and gradient boosting techniques, additional enhancements drove the accuracy to 87%, with CatBoost and LightGBM excelling among others. These results highlight the importance of frequency-domain characteristics and model optimization in increasing fault detection dependability. In conclusion, this study helps to encourage the inclusion of intelligent monitoring systems into predictive maintenance pipelines, therefore prolonging the lifetime of industrial equipment and reducing operational downtime.

Keywords-predictive maintenance; vibration signal processing; frequency-domain analysis; ensemble learning algorithms; feature engineering

I. INTRODUCTION

Condition-based maintenance techniques have been widely adopted in industrial systems to enhance operational reliability and energy efficiency [1]. Induction motors are commonly used in industrial processes due to their durability, simplicity, and cost-effectiveness [2]. Although they have benefits, they are nonetheless prone to several flaws, such as bearing wear, rotor bar problems, and electrical imbalances, which, if left unnoticed, can cause catastrophic failures and unscheduled downtime [3]. Maintaining system integrity and operational continuity thus depends on early discovery and precise characterization of such defects [4].

Using high-frequency vibration data to consistently identify motor failures using intelligent algorithms, this work aimed to resolve a fundamental difficulty in industrial diagnostics. Conventional approaches, such as thresholding methods or rule-based monitoring, sometimes struggle to adapt to varying fault types and complex signal patterns [5]. Machine Learning (ML) has become a potent instrument for analyzing such challenging data in recent years [6]. For fault detection activities, several researchers have investigated the application of ML models, such as K-Nearest Neighbors (KNN) [7], Random Forest (RF) [8], Decision Trees [9], and ensemble approaches such as GradientBoosting (GB) [10], Adaptive Boosting (AdaBoost) [11], Extreme Gradient Boosting (XGBoost) [12], Light Gradient Boosting Machine (LGBM) [13], and Categorical Boosting (CatBoost) [14]). In controlled situations, models incorporating time-domain statistical characteristics have shown poor performance [15]. However, many current methods either ignore frequency-domain properties or neglect model adjustment, therefore restricting their generalizability and accuracy in practical uses [16].

The main goal of this work is to investigate the use of both time- and frequency-domain features extracted from vibration signals to improve the relative performance of ML classifiers in diagnosing induction motor defects. Three experimental situations were methodically investigated: (i) Simple statistical feature-based baseline multiclass categorization; (ii) Binary classification with expanded Fast Fourier Transform (FFT)-based features; (iii) GridSearchCV [17] optimization of advanced gradient boosting models such as LGBM and Catboost. One of the main limitations of previous works is the insufficient use of the frequency spectrum of vibration signals and the ignoring of the parameter adjustment to achieve higher classifier performance [18].

This work presents a novel approach to developing a robust and scalable fault diagnosis system by combining hyperparameter-optimized classifiers with time-frequency feature engineering. Starting with real-world data acquisition in TDMS form from a National Instruments DAQ system [19], the proposed pipeline proceeds with signal processing [20], feature extraction [21], class balancing through the Synthetic Minority Oversampling Technique (SMOTE) [22], and thorough evaluation of many classifiers using comprehensive metrics [23]. These devices are prone to several faults, particularly inter-turn short circuit defects of varying severity, as investigated in this study.

Unlike prior studies that often rely solely on time-domain features or overlook parameter tuning, this work addresses this gap by integrating frequency-domain features with optimized ensemble models. The contribution of this study lies in: (i) systematically comparing time-, frequency-, and combined-domain features; (ii) demonstrating the effect of data balancing and scaling; (iii) highlighting the role of hyperparameter optimization in boosting diagnostic accuracy. Thus, this study forms a reproducible framework for predictive maintenance applications.

In brief, the results show that whilst the combination of FFT features and binary classification increases the accuracy to ~80%, models trained just on time-domain features perform poorly in multiclassification (accuracy ~20%). With CatBoost and LGBM attaining over 87% accuracy and greater R^2 scores, hyperparameter tuning and boosting-based classifiers mark the most important development. These results emphasize the need for frequency-domain information in predictive maintenance as well as the need for proper model selection and adjustment. This study suggests an extendable and optimal framework for vibration-based defect diagnostics in induction motors. Combining signal processing, feature engineering, and ML produces a practical, generalizable, and accurate predictive maintenance solution. The insights gained can direct future studies on industrial IoT applications and smart condition monitoring systems.

II. RESEARCH METHODOLOGY

This study uses a public dataset comprising vibration signals recorded in the z-direction of a 1.0 kW induction motor in several short circuit fault scenarios [24]. Each file matched a particular fault severity level in data obtained with a National Instruments DAQ system and kept in TDMS format. Eight conditions are illustrated, with labels ranging from 0 to 7 (Table I).

TABLE I. FAULT CONDITIONS DATASET

Label	File Name	Fault Condition	Severity (%)
0	1000W_2_26.tdms	Inter-turn short circuit fault	2.26
1	1000W_2_70.tdms	Inter-turn short circuit fault	2.70
2	1000W_3_35.tdms	Inter-turn short circuit fault	3.35
3	1000W_4_41.tdms	Inter-turn short circuit fault	4.41
4	1000W_6_48.tdms	Inter-turn short circuit fault	6.48
5	1000W_12_17.tdms	Inter-turn short circuit fault	12.17
6	1000W_21_69.tdms	Inter-turn short circuit fault	21.69
7	1000W_0_00.tdms	Normal (Healthy)	0.00

Label 7 refers to the healthy state, including vibration data for the motor running fault-free. This provides the standard for comparison. Labels 0 through 6 indicate different degrees of inter-turn short circuit failures, increasing in severity. Label 0 specifically captures 2.26% severity early-stage malfunction behavior. At 2.70%, label 1 exhibits a somewhat more developed fault. Label 2 rises to 3.35%. Label 3 at 4.41% and label 4 at 6.48% stand for mid-level fault conditions. Label 5 with a 12.17% degree and label 6 with the greatest degree of 21.69% reflect more severe circumstances.

Both binary and multiclass categorization are made possible by these labels. All eight labels in the multiclass system help to categorize fault severities. Under the Fault category (class 0), labels 0 through 6 are classified in the binary classification scenarios, and label 7 is handled as the Normal class (class 1). This enables the development of more pragmatic fault/no-fault detectors fit for real-time industrial deployment as well as thorough diagnostic models.

Figure 1 shows, spanning Label 0 to Label 7, a plot of vibration signals arranged by fault severity labels. Under the given circumstances of inter-turn short circuit defects, each colored segment shows vibration data gathered from an induction motor with increasing intensity from left to right. The y-axis shows the vibration amplitude in the z-direction, and the x-axis indicates the sample index, illustrating the evolution of recorded data points over time. This graph shows the slow change of fault properties. Labels 0 to 2 show lower severity circumstances, with somewhat steady and low-amplitude vibration patterns. Signal amplitude and variability clearly climb as fault severity increases (Labels 3 through 6), suggesting increasingly severe mechanical or electrical disturbances inside the motor windings. Reflecting constant motor running, the last section, Label 7 (gray), corresponds to the healthy condition and displays a notable decrease in vibration magnitude and noise.

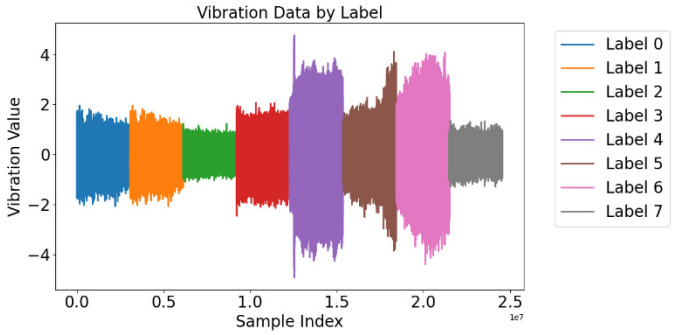

Fig. 1. Vibration dataset distributions.

Figure 2 shows a histogram of vibration levels taken from the complete induction motor dataset under several running situations. Raw vibration amplitudes are crucially important for feature extraction and model training in fault diagnosis activities. The y-axis denotes the frequency, that is, the number of occurrences of every vibration amplitude in the dataset. The x-axis represents the range of vibration values. The histogram shows that, centered on zero, the vibration data follow a somewhat Gaussian (normal) distribution. With a high peak at 0, most vibration readings are low in magnitude as expected during normal operation or low-severity fault conditions, and most of the data falls between roughly -1.5 and +1.5. However, especially toward negative values, the distribution shows some asymmetry and long tails, which imply the possibility of sporadic strong-amplitude oscillations. These anomalies might match periods when the motor suffered transitory mechanical fluctuations or severe defects. This fluctuation justifies rolling statistical features (such as mean, standard deviation, peak, and min) and FFT analysis to identify these deviations.

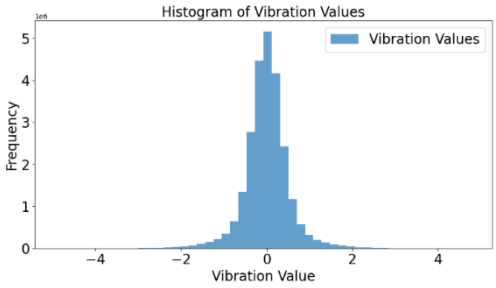

Fig. 2. Dataset distribution histogram.

In ML environments, this histogram justifies the application of SMOTE, since the imbalance in signal characteristics could lead to skewed learning if not addressed, and confirms the decision to apply feature scaling (e.g., StandardScaler). The normal form of the distribution also helps to reassure one that the dataset does not show significant bias or irregular sampling errors. Three experimental setups were used (Table II) to methodically assess the effects of feature complexity, classification method, and model optimization on the accuracy of induction motor failure diagnosis.

TABLE II. RESEARCH OVERVIEW

Aspect	Setup 1	Setup 2	Setup 3
Task type	Multiclass classification (7 labels)	Binary classification (Fault vs Normal)	Binary classification (Fault vs Normal)
Feature engineering	Time-domain features: Vibration, Vibration_Mean, Vibration_Std	Time-domain + Frequency-domain: Vibration_Peak, Vibration_Min, FFT_Power, FFT_Dominant_Freq	Time-domain + Frequency-domain: Vibration_Peak, Vibration_Min, FFT_Power, FFT_Dominant_Freq
FFT features	No	Yes	Yes
Sampling strategy	Downsampled to 0.05%		
Imbalance handling	SMOTE applied		
Models used	KNN, RandomForest, GradientBoosting, AdaBoost, XGBoost, LightGBM, CatBoost		
Hyperparameter tuning	No tuning	No tuning	GridSearchCV
Output Metrics	Accuracy, MSE, RMSE, R^2		

Each motor condition, seven fault severities and one healthy, was treated as a distinct label. Setup 1 focused on multiclassification. Here, feature engineering depended only on fundamental time-domain characteristics, such as raw vibration signals and rolling statistics, mean, and standard deviation, without using frequency-domain data. The goal was to provide a baseline performance without further changes, using basic, simply extractable characteristics. Despite its simplicity, this configuration helped show the limits of time-domain-only methods in differentiating complicated failure behaviors.

By grouping labels 0 through 6 (fault cases) into a single Fault class and label 7 in Normal (healthy condition), Setup 2 reformed the task into a binary classification. This more pragmatic approach captures actual maintenance requirements, that is, how to tell bad from good machinery. More importantly, by merging time- and frequency-domain features, Setup 2 brought a richer feature set. Using a rolling window approach, additional features were calculated, such as peak vibration, minimum vibration, FFT-derived total power, and dominant frequency [25]. The peak vibration value was calculated using (1), where x_t is the instantaneous vibration signal. The total spectral power was obtained using (2), where X_k is the Fourier transform magnitude at frequency bin k. This feature quantifies the overall energy content of the vibration signal in the frequency domain. The dominant frequency, which represents the most prominent spectral component, was defined as in (3), where f_{dom} identifies the frequency corresponding to the maximum spectral amplitude, indicating the most fault-sensitive frequency in the signal. FFT characteristics let models detect fault-related frequency signatures sometimes missed in raw time-domain signals [26]. However, just as in Setup 1, no hyperparameter adjustment was performed, therefore restricting the potential of some models.

$$x_{peak} = \max(x_{t-N+1}, \dots, x_t), x_{min} = \min(x_{t-N+1}, \dots, x_t) \quad (1)$$

$$P = \sum_{k=1}^{N} |X_k|^2 \quad (2)$$

$$f_{\text{dom}} = \arg\max_k |X_k| \quad (3)$$

Retaining the same binary classification job and feature set, Setup 3 extended the previous setup using GridSearchCV [27] to optimize hyperparameters, improving the parameters of algorithms such as KNN, Random Forest [28], Gradient Boosting, AdaBoost, LightGBM, and Catboost [29]. Adapting every model better to the properties of the extracted features, tuning greatly improved performance [30]. By integrating advanced ensemble learners, including XGBoost, LightGBM, and Catboost, well-regarded for their predictive strength and efficiency on structured data, Setup 3 assessed a larger model pool.

To reduce computational strain and maintain data variability across all configurations, the dataset was downsampled to 0.05% of its original size. For the common problem of class imbalance, particularly in binary classification, SMOTE [31] was used on the training set in every case. Accuracy, Mean Squared Error (MSE), Mean Absolute Percentage Error (MAPE), Root Mean Squared Error (RMSE), and R² were among the whole set of measures used consistently to evaluate model performance [32]. These measures revealed information on both the generalizing capacity of the models across different operational situations and classification accuracy [33].

In MSE (4), y_i and $\hat{y}_i$ are the actual and predicted values, and n is the number of samples. MSE measures the average squared difference between predictions and ground truth. MAPE (5) evaluates the relative size of prediction errors as a percentage of the actual values. RMSE (6) provides an interpretable error magnitude in the same unit as the target variable. Finally, in the Coefficient of Determination (R^2) (7), $\hat{y}$ is the mean of the actual values. R^2 quantifies the proportion of variance in the dataset explained by the model, with values closer to 1 indicating better predictive performance.

$$\text{MSE} = \frac{1}{n}\sum_{i=1}^{n}(y_i - \hat{y}_i)^2 \quad (4)$$

$$\text{MAPE} = \frac{100}{n}\sum_{i=1}^{n}\left|\frac{y_i - \hat{y}_i}{y_i}\right| \quad (5)$$

$$\text{RMSE} = \sqrt{\text{MSE}} \quad (6)$$

$$R^2 = \frac{\sum(y_i - \hat{y}_i)^2}{\sum(y_i - \bar{y})^2} \quad (7)$$

III. RESULTS AND DISCUSSION

Using GridSearchCV, the outcomes of the hyperparameter tuning process expose insights into the performance potential of several ML classifiers when optimized for fault diagnostics in induction motors (Table III). Each model was cross-validated to find the optimal parameter configuration and associated accuracy. Using the Manhattan distance metric, with three neighbors and distance-based weighting, the KNN classifier achieved a cross-validation accuracy of 81.13%. This result implies that for differentiating between defective and healthy motor states, local proximity patterns in the vibration feature space are rather helpful. When the data distribution is well-mannered and suitably sampled, KNN's simplicity and non-parametric character help it to be efficient.

TABLE III. GRIDSEARCHCV RESULTS

Model	Best parameters	Best cross-validation accuracy
KNN	{'metric': 'manhattan', 'n_neighbors': 3, 'weights': 'distance'}	0.8113
RF	{'max_depth': 20, 'min_samples_split': 2, 'n_estimators': 100}	0.7918
GB	{'learning_rate': 0.2, 'max_depth': 7, 'n_estimators': 200}	0.8422
AdaBoost	{'learning_rate': 1.0, 'n_estimators': 200}	0.6264
LGBM	{'learning_rate': 0.2, 'max_depth': 10, 'n_estimators': 500}	0.8492
CatBoost	{'depth': 8, 'iterations': 500, 'learning_rate': 0.2}	0.8537

In Setup 1 (Table IV), all classifiers were assessed on the raw imbalanced dataset without standardization or class balancing. The performance of all models was clearly inadequate. For most models, accuracy remained below 21%, with KNN scoring just 19.49% and CatBoost plummeting to 10.90%, signifying a significant bias towards the majority class. Furthermore, indicating notable prediction errors, RMSE fluctuated between 30 and 42, while MSE ranged from 91.118 to 178.417. A similar situation was noticed for LGBM and Catboost. Most remarkably, the R^2 scores were strongly negative for every model, with CatBoost yielding a disastrous -248.85, meaning that all models performed worse than a horizontal mean forecast. This setup clearly shows that, particularly in fault detection situations where class imbalance is evident, raw vibration data without normalization and class balancing does not offer sufficient signal quality or distribution for meaningful learning.

TABLE IV. SETUP 1 EXPERIMENTAL RESULTS

Model	Accuracy	MSE	RMSE	R^2
KNN	0.1949	108.805	32.986	-10.632
RF	0.2038	116.350	34.110	-12.062
GB	0.1941	105.351	32.458	-0.9977
AdaBoost	0.1877	137.722	37.111	-16.115
LGBM	0.1977	91.118	30.185	-0.7815
CatBoost	0.1090	178.417	42.239	-248.85

By standardizing the features and tackling class imbalance with SMOTE, Setup 2 (Table V) yielded performance improvements. KNN displayed amazing improvement, with 79.98% accuracy and a far reduced MSE of 0.2002. Likewise, LGBM and CatBoost achieved accuracies of 68.52% and 74.25% respectively. Reflecting substantial learning, RMSE declined greatly to about 0.5, and R^2 values were close to zero. These results show that equalizing the class distribution and standardizing the input features greatly improve the generalizing and defect-detecting capacity of the model. Still, certain gradient boosting models suffered from overfitting or unstable computations, most likely because of outlier sensitivity in the resampled data.

TABLE V. SETUP 2 EXPERIMENTAL RESULTS

Model	Accuracy	MSE	RMSE	R^2
KNN	0.7998	0.2002	0.4474	0.1992
RF	0.6787	0.3213	0.5669	-0.2854
GB	0.7042	0.2958	0.5439	-0.1834
AdaBoost	0.6174	0.3826	0.6185	-0.5305
LGBM	0.6852	0.3147	0.5610	-0.2591
CatBoost	0.7425	0.2574	0.5074	-0.0299

Further preprocessing improvements in Setup 3 (Table VI), along with incorporating well-tuned feature engineering such as FFT power and peak detection, produced the best overall model performance. Although all models improved, gradient boosting-based classifiers outperformed others. Closely followed by LGBM at 87.16%, CatBoost obtained the greatest accuracy of 87.28%, with GB at 86.60%. With values as low as 0.1272 and 0.3567, respectively, these models exhibited the lowest MSE and RMSE. Most notably, R^2 scores turned positive and high up to 0.4911 for CatBoost, indicating a great correlation between expected and actual labels. These results verify that, particularly for binary fault classification using vibration signals, a combination of feature extraction, scaling, data balancing, and hyperparameter tuning significantly improves predictive power.

TABLE VI. SETUP 3 EXPERIMENTAL RESULTS

Model	Accuracy	MSE	MAPE	RMSE	R^2
KNN	0.8492	0.1508	4.99e+14	0.3884	0.3966
RF	0.8101	0.1899	6.55e+14	0.4358	0.2404
GB	0.8660	0.1340	2.73e+14	0.3661	0.4640
AdaBoost	0.6211	0.3789	1.43e+15	0.6155	-0.5155
LGBM	0.8716	0.1284	2.80e+14	0.3583	0.4864
CatBoost	0.8728	0.1272	2.63e+14	0.3567	0.4911

With 100 trees, a maximum depth of 20, and a minimum sample split of 2, the RF model achieved a rather lower accuracy of 79.18%, with hyperparameter optimization. This suggests that although the model's performance is limited by bootstrapped tree diversity, deeper trees help it to capture intricate connections between time-frequency characteristics. Using 200 estimators, a max depth of 7, and a learning rate of 0.2, the GB model achieved 84.22% accuracy. Especially in fault detection situations with complex signal patterns, this shows how well boosting techniques successively correct weak learners to produce a stronger ensemble. In comparison, AdaBoost underperformed compared to other boosting models, obtaining only 62.64% accuracy at its highest with 200 estimators and a learning rate of 1.0. One explanation may be that its sensitivity to noise and its less flexible boosting structure are often surpassed by GB methods in complicated datasets. With an accuracy of 84.92%, tuned with 500 estimators, max depth of 10, and a learning rate of 0.2, LGBM really shone, showing that its quick training and leaf-wise tree growth approach is well-suited for large-scale high-dimensional data, making it a great choice for real-time diagnostics. With 500 iterations, a depth of 8, and a learning rate of 0.2, the CatBoost model finally ranked highest among all models with an accuracy of 85.37%. Although not utilized here, CatBoost's exceptional handling of categorical data, built-in regularization, and robustness to overfitting help to explain its great performance and prove its applicability for industrial fault classification tasks.

These findings highlight the need for feature richness and hyperparameter optimization to achieve high diagnostic accuracy. They also underscore the relative benefits of modern ensemble models such as LGBM and Catboost in vibration-based predictive maintenance applications. Future work should further compare models trained with and without hyperparameter optimization, and advanced search methods, such as Bayesian optimization, are recommended to confirm these findings.

In addition to conventional evaluation criteria, such as accuracy and error rates, this study evaluated every classifier based on inference time and model size, two important considerations for practical application in industrial settings [34]. Measured in seconds, inference time is the process by which a trained model generates predictions on fresh, unaccustomed input [35]. Faster decision-making implied by shorter inference time is especially important in time-sensitive applications, including early failure detection and real-time motor monitoring [36]. GB showed the fastest inference among the models, at about 0.0088 s, with CatBoost and LightGBM following. Conversely, KNN's lazy learning style, which depends on complete dataset comparisons during prediction, had the longest inference time (0.0623 s).

Reported in kilobytes (KB), the model size tells the trained model's storage footprint. Systems with limited resources, such as embedded devices or edge computing units, often employed in predictive maintenance systems, depend on this measure. Reflecting the overhead related to storing several decision trees, RF had the largest model size at 2910.63 KB, while AdaBoost had the shortest model size at just 63.91 KB. With rather small model sizes (337.19 KB and 116.82 KB, respectively), LightGBM and Catboost presented a good trade-off between performance and comparatively compact sizes (Table VII).

TABLE VII. SETUP 3 EXPERIMENTAL RESULTS

Model	Inference time (s)	Model size (KB)
KNN	0.0623	1716.44
RF	0.0425	2910.63
GB	0.0088	462.85
AdaBoost	0.0549	63.91
LGBM	0.0461	337.19
CatBoost	0.0230	116.82

Together, inference time and model size offer useful insights that complement accuracy, therefore guiding engineers and system designers in choosing models not only for precision but also for efficiency and deployability in limited settings.

IV. CONCLUSION

This work marks significant progress in the field of induction motor failure diagnostics by combining hyperparameter-optimized ML models with frequency-domain characteristics into a single predictive maintenance system. Unlike previous techniques that may depend on basic statistical analysis or untuned models, this study developed a more rigorous and scalable approach capable of diagnosing both mild and severe inter-turn short circuit problems using real-world vibration data. The fundamental scientific contribution is in verifying that time-frequency feature fusion, especially the inclusion of FFT power and dominant frequency, allows a more robust description of motor behavior under fault conditions. The results showed that not only feature richness, but also model architecture and parameter adjustment, assess model performance over three experimental scenarios. After applying GridSearchCV, the better results from LGBM and Catboost highlight the need for adaptive learning frameworks to handle challenging high-dimensional sensor data.

In addition, this study provides a reproducible template for academics and practitioners wishing to use smart diagnostic systems in industrial situations, which includes preprocessing of TDMS-format vibration data, SMOTE for class balance, and stringent assessment metrics. With possible uses in more general Industry 4.0 systems, these results promote a change from reactive maintenance to condition-based monitoring. Extending this technology to online, real-time defect detection systems, including more sensor axes and combining domain adaptation techniques to generalize models across various motor types and operational loads, will be the main focus of future study. Using deep learning architectures, such as 1D CNNs and transformer-based time-series models, to automate feature extraction and further increase scalability is another exciting area. This work significantly helps shape intelligent industrial automation by providing the foundation for more precise, interpretable, and responsive motor health monitoring systems.

ACKNOWLEDGMENT

The authors wish to thank the Mahasarakham University staff and professors for their ongoing support, technical help, and resource availability throughout the project. This research was made possible in great part by their direction and encouragement.

REFERENCES

[1] A. Acernese, C. Del Vecchio, M. Tipaldi, N. Battilani, and L. Glielmo, "Condition-based maintenance: an industrial application on rotary machines," *Journal of Quality in Maintenance Engineering*, vol. 27, no. 4, pp. 565–585, Oct. 2021, https://doi.org/10.1108/JQME-10-2019-0101.

[2] D. Tiwari, J. Miscandlon, A. Tiwari, and G. W. Jewell, "A Review of Circular Economy Research for Electric Motors and the Role of Industry 4.0 Technologies," *Sustainability*, vol. 13, no. 17, Aug. 2021, Art. no. 9668, https://doi.org/10.3390/su13179668.

[3] F. Xu *et al.*, "A review of bearing failure Modes, mechanisms and causes," *Engineering Failure Analysis*, vol. 152, Oct. 2023, Art. no. 107518, https://doi.org/10.1016/j.engfailanal.2023.107518.

[4] F. A. Costa De Oliveira, F. S. Torres, and A. Garcia-Ortiz, "Recent Advances in Sensor Integrity Monitoring Methods—A Review," *IEEE Sensors Journal*, vol. 22, no. 11, pp. 10256–10279, Jun. 2022, https://doi.org/10.1109/JSEN.2022.3169659.

[5] X. Yan, N. Li, Y. Yu, W. He, and D. Wang, "A Bearing Fault Diagnosis Method Based on Hierarchical Belief Rule Base With Power Set," *IEEE Access*, vol. 13, pp. 70324–70339, 2025, https://doi.org/10.1109/ACCESS.2025.3558798.

[6] A. A. Soomro *et al.*, "Insights into modern machine learning approaches for bearing fault classification: A systematic literature review," *Results in Engineering*, vol. 23, Sep. 2024, Art. no. 102700, https://doi.org/10.1016/j.rineng.2024.102700.

[7] Q. Wang, S. Wang, B. Wei, W. Chen, and Y. Zhang, "Weighted K-NN Classification Method of Bearings Fault Diagnosis With Multi-Dimensional Sensitive Features," *IEEE Access*, vol. 9, pp. 45428–45440, 2021, https://doi.org/10.1109/ACCESS.2021.3066489.

[8] S. S. Roy, S. Dey, and S. Chatterjee, "Autocorrelation Aided Random Forest Classifier-Based Bearing Fault Detection Framework," *IEEE Sensors Journal*, vol. 20, no. 18, pp. 10792–10800, Sep. 2020, https://doi.org/10.1109/JSEN.2020.2995109.

[9] I. D. Mienye and N. Jere, "A Survey of Decision Trees: Concepts, Algorithms, and Applications," *IEEE Access*, vol. 12, pp. 86716–86727, 2024, https://doi.org/10.1109/ACCESS.2024.3416838.

[10] F. Huber, A. Yushchenko, B. Stratmann, and V. Steinhage, "Extreme Gradient Boosting for yield estimation compared with Deep Learning approaches," *Computers and Electronics in Agriculture*, vol. 202, Nov. 2022, Art. no. 107346, https://doi.org/10.1016/j.compag.2022.107346.

[11] T. Toharudin *et al.*, "Boosting Algorithm to Handle Unbalanced Classification of $PM_{2.5}$ Concentration Levels by Observing Meteorological Parameters in Jakarta-Indonesia Using AdaBoost, XGBoost, CatBoost, and LightGBM," *IEEE Access*, vol. 11, pp. 35680–35696, 2023, https://doi.org/10.1109/ACCESS.2023.3265019.

[12] Pamir, N. Javaid, M. Akbar, A. Aldegheishem, N. Alrajeh, and E. A. Mohammed, "Employing a Machine Learning Boosting Classifiers Based Stacking Ensemble Model for Detecting Non Technical Losses in Smart Grids," *IEEE Access*, vol. 10, pp. 121886–121899, 2022, https://doi.org/10.1109/ACCESS.2022.3222883.

[13] J. Yan *et al.*, "LightGBM: accelerated genomically designed crop breeding through ensemble learning," *Genome Biology*, vol. 22, no. 1, Dec. 2021, Art. no. 271, https://doi.org/10.1186/s13059-021-02492-y.

[14] M. Mao *et al.*, "Application of FCEEMD-TSMFDE and adaptive CatBoost in fault diagnosis of complex variable condition bearings," *Scientific Reports*, vol. 14, no. 1, Dec. 2024, Art. no. 30448, https://doi.org/10.1038/s41598-024-78845-x.

[15] Z. Wang *et al.*, "Rolling bearing fault diagnosis method using time-frequency information integration and multi-scale TransFusion network," *Knowledge-Based Systems*, vol. 284, Jan. 2024, Art. no. 111344, https://doi.org/10.1016/j.knosys.2023.111344.

[16] A. Keil *et al.*, "Recommendations and publication guidelines for studies using frequency domain and time-frequency domain analyses of neural time series," *Psychophysiology*, vol. 59, no. 5, May 2022, Art. no. e14052, https://doi.org/10.1111/psyp.14052.

[17] T. Alshammari, "Using Artificial Neural Networks with GridSearchCV for Predicting Indoor Temperature in a Smart Home," *Engineering, Technology & Applied Science Research*, vol. 14, no. 2, pp. 13437–13443, Apr. 2024, https://doi.org/10.48084/etasr.7008.

[18] A. A. Jaber, "Diagnosis of Bearing Faults Using Temporal Vibration Signals: A Comparative Study of Machine Learning Models with Feature Selection Techniques," *Journal of Failure Analysis and Prevention*, vol. 24, no. 2, pp. 752–768, Apr. 2024, https://doi.org/10.1007/s11668-024-01883-0.

[19] J. Kneifel, R. Roj, H. B. Woyand, R. Theiß, and P. Dültgen, "An IIoT-Device for Acquisition and Analysis of High-Frequency Data Processed by Artificial Intelligence," *IoT*, vol. 4, no. 3, pp. 244–264, Jul. 2023, https://doi.org/10.3390/iot4030013.

[20] S. Sudirman, F. Natalia, A. Sophian, and A. Ashraf, "Pulsed Eddy Current signal processing using wavelet scattering and Gaussian process regression for fast and accurate ferromagnetic material thickness measurement," *Alexandria Engineering Journal*, vol. 61, no. 12, pp. 11239–11250, Dec. 2022, https://doi.org/10.1016/j.aej.2022.04.028.

[21] C. Zhang, A. A. Mousavi, S. F. Masri, G. Gholipour, K. Yan, and X. Li, "Vibration feature extraction using signal processing techniques for structural health monitoring: A review," *Mechanical Systems and Signal Processing*, vol. 177, Sep. 2022, Art. no. 109175, https://doi.org/10.1016/j.ymssp.2022.109175.

[22] D. Dablain, B. Krawczyk, and N. V. Chawla, "DeepSMOTE: Fusing Deep Learning and SMOTE for Imbalanced Data," *IEEE Transactions on Neural Networks and Learning Systems*, vol. 34, no. 9, pp. 6390–6404, Sep. 2023, https://doi.org/10.1109/TNNLS.2021.3136503.

[23] A. De La Cruz Huayanay, J. L. Bazán, and C. M. Russo, "Performance of evaluation metrics for classification in imbalanced data," *Computational Statistics*, Aug. 2024, https://doi.org/10.1007/s00180-024-01539-5.

[24] W. Jung, S. H. Yun, Y. S. Lim, S. Cheong, and Y. H. Park, "Vibration and current dataset of three-phase permanent magnet synchronous motors with stator faults," *Data in Brief*, vol. 47, Apr. 2023, Art. no. 108952, https://doi.org/10.1016/j.dib.2023.108952.

[25] S. Gawde, S. Patil, S. Kumar, P. Kamat, K. Kotecha, and S. Alfarhood, "Explainable Predictive Maintenance of Rotating Machines Using LIME, SHAP, PDP, ICE," *IEEE Access*, vol. 12, pp. 29345–29361, 2024, https://doi.org/10.1109/ACCESS.2024.3367110.

[26] Y. Wang, L. Zheng, Y. Gao, and S. Li, "Vibration Signal Extraction Based on FFT and Least Square Method," *IEEE Access*, vol. 8, pp. 224092–224107, 2020, https://doi.org/10.1109/ACCESS.2020.3044149.

[27] G. N. Ahmad, H. Fatima, S. Ullah, A. Salah Saidi, and Imdadullah, "Efficient Medical Diagnosis of Human Heart Diseases Using Machine Learning Techniques With and Without GridSearchCV," *IEEE Access*, vol. 10, pp. 80151–80173, 2022, https://doi.org/10.1109/ACCESS.2022.3165792.

[28] P. Thavitchasri, D. Maneetham, and P. N. Crisnapati, "Intelligent Surface Recognition for Autonomous Tractors Using Ensemble Learning with BNO055 IMU Sensor Data," *Agriculture*, vol. 14, no. 9, Sep. 2024, Art. no. 1557, https://doi.org/10.3390/agriculture14091557.

[29] M. M. Ghiasi and S. Zendehboudi, "Application of decision tree-based ensemble learning in the classification of breast cancer," *Computers in Biology and Medicine*, vol. 128, Jan. 2021, Art. no. 104089, https://doi.org/10.1016/j.compbiomed.2020.104089.

[30] N. Ding *et al.*, "Parameter-efficient fine-tuning of large-scale pre-trained language models," *Nature Machine Intelligence*, vol. 5, no. 3, pp. 220–235, Mar. 2023, https://doi.org/10.1038/s42256-023-00626-4.

[31] D. Elreedy, A. F. Atiya, and F. Kamalov, "A theoretical distribution analysis of synthetic minority oversampling technique (SMOTE) for imbalanced learning," *Machine Learning*, vol. 113, no. 7, pp. 4903–4923, Jul. 2024, https://doi.org/10.1007/s10994-022-06296-4.

[32] X. Li and X. Zhang, "A comparative study of statistical and machine learning models on carbon dioxide emissions prediction of China," *Environmental Science and Pollution Research*, vol. 30, no. 55, pp. 117485–117502, Oct. 2023, https://doi.org/10.1007/s11356-023-30428-5.

[33] P. Zhang *et al.*, "Improving generalisation and accuracy of on-line milling chatter detection via a novel hybrid deep convolutional neural network," *Mechanical Systems and Signal Processing*, vol. 193, Jun. 2023, Art. no. 110241, https://doi.org/10.1016/j.ymssp.2023.110241.

[34] R. Panigrahi *et al.*, "Performance Assessment of Supervised Classifiers for Designing Intrusion Detection Systems: A Comprehensive Review and Recommendations for Future Research," *Mathematics*, vol. 9, no. 6, Mar. 2021, Art. no. 690, https://doi.org/10.3390/math9060690.

[35] H. Tian and A. Ji, "Real-Time Adaptive Tractor Ride Comfort Adjustment System Based on Machine Learning Method," *IEEE Access*, vol. 13, pp. 3274–3283, 2025, https://doi.org/10.1109/ACCESS.2024.3522959.

[36] T. Coito, B. Firme, M. S. E. Martins, S. M. Vieira, J. Figueiredo, and J. M. C. Sousa, "Intelligent Sensors for Real-Time Decision-Making," *Automation*, vol. 2, no. 2, pp. 62–82, May 2021, https://doi.org/10.3390/automation2020004.